Electronic Supplementary Material (ESI) for Journal of Materials Chemistry C.

Supporting Information

An all white magnet by combination of electronic properties of a white light emitting MOF with strong magnetic particle systems

Marcel T. Seuffert,[θa] Susanne Wintzheimer,[θb] Maximilian Oppmann,[c] Tim Granath,[b] Johannes Prieschl,[b] Anas Alrefai,[d] Hans-Jürgen Holdt,[d] Klaus Müller-Buschbaum,*[ae] Karl Mandel*[bc]

[a] Institute of Inorganic and Analytical Chemistry, Justus-Liebig-University Giessen, Heinrich-Buff-Ring 17, D35392 Gießen, Germany.
[b] Friedrich-Alexander University Erlangen-Nürnberg (FAU), Department of Chemistry and Pharmacy, Professorship for Inorganic Chemistry, Egerlandstraße 1, 91058 Erlangen, Germany.
[c] Fraunhofer Institute for Silicate Research, ISC, Neunerplatz 2, D97082 Würzburg, Germany.
[d] Institute of Chemistry, University of Potsdam, Karl-Liebknecht-Straße 24-25, D14476 Golm, Germany.
[e] Center for Materials Research (LAMA), Justus-Liebig-University Giessen, Heinrich-Buff-Ring 16, D35392 Gießen, Germany.
* K.M.-B.: kmbac@uni-giessen.de; K.M.: karl.mandel@fau.de
[θ] these authors contributed equally to this work.

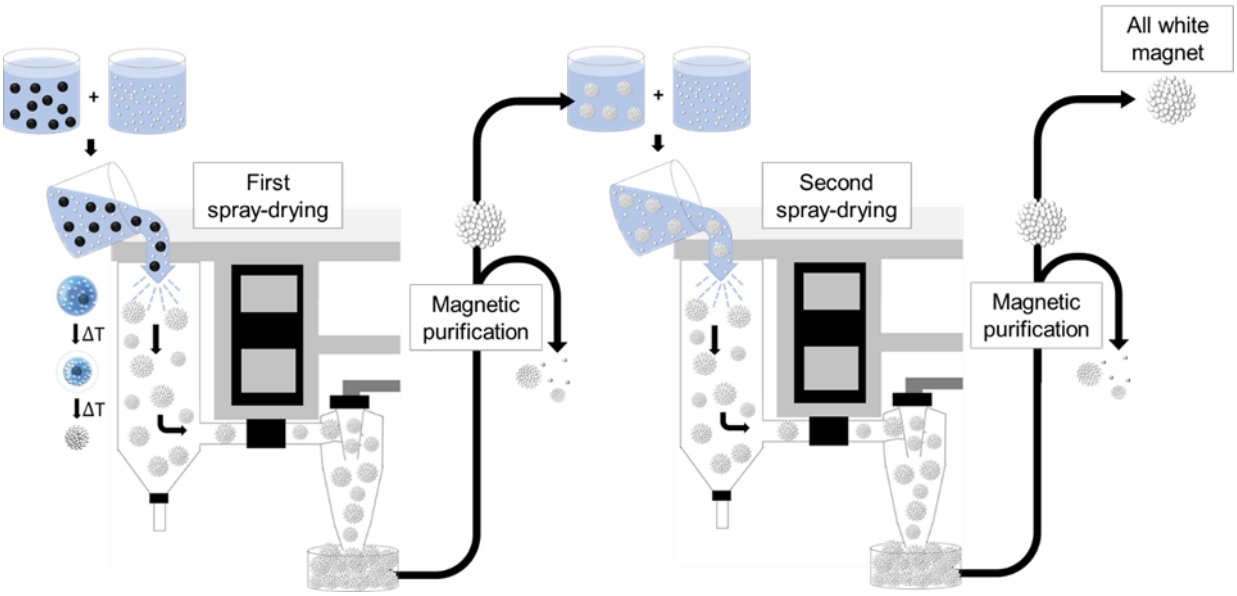

Figure S1. Principle scheme of the synthesis setup for the white micro magnet (WI and WO).The core material is covered by titania pigments by two spray-drying cycles followed by magnetic purification in order to remove non-magnetic side-products.

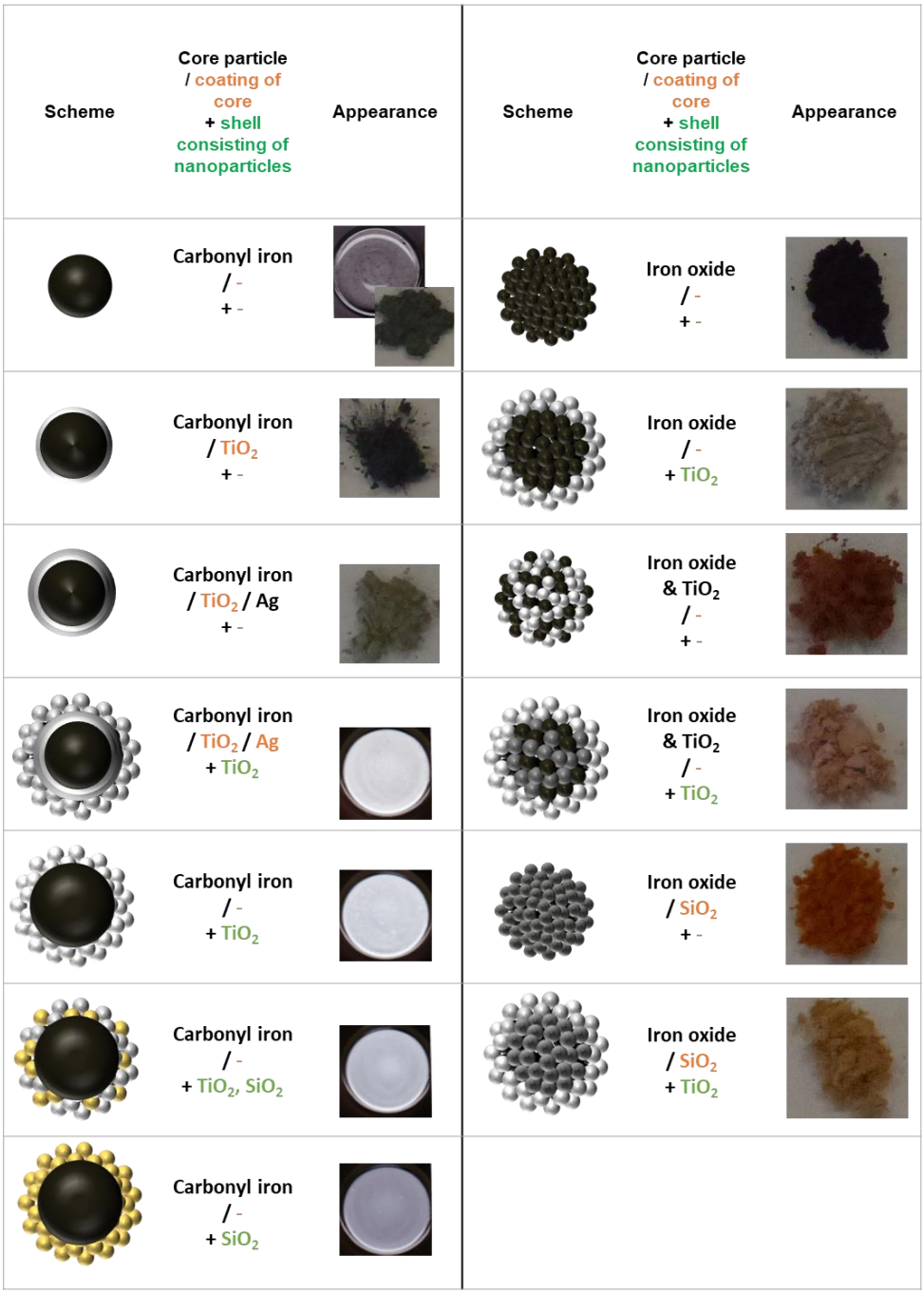

Figure S2. The creation of magnetic more or less whitish core-shell supraparticles via spray-drying. The choice of building blocks including the magnetic core material, titania and silica nanoparticles, addition of optional pre-treatment steps such as a coating with Ag or silica and a variation of the many spray-drying parameters lead to an enormous variety in terms of color appearance of obtained complex microparticles as shown in this figure exemplarily for several combinations and procedures.

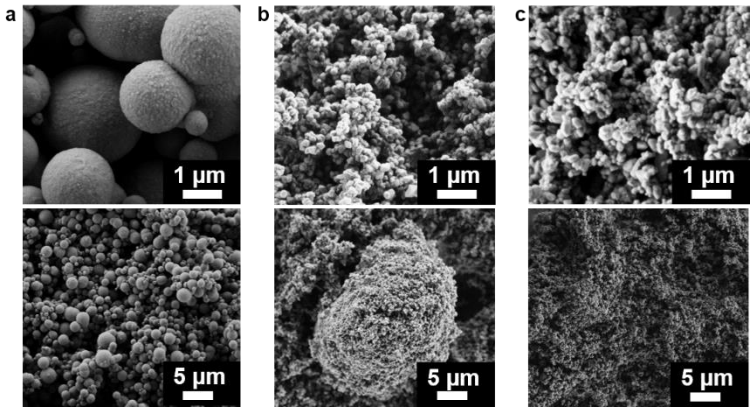

Figure S3. Scanning electron microscopy of precursor particles. Scanning electron micrographs of α-iron (a) and iron oxide particles (b), as well as TiO_2 nanoparticles (c).

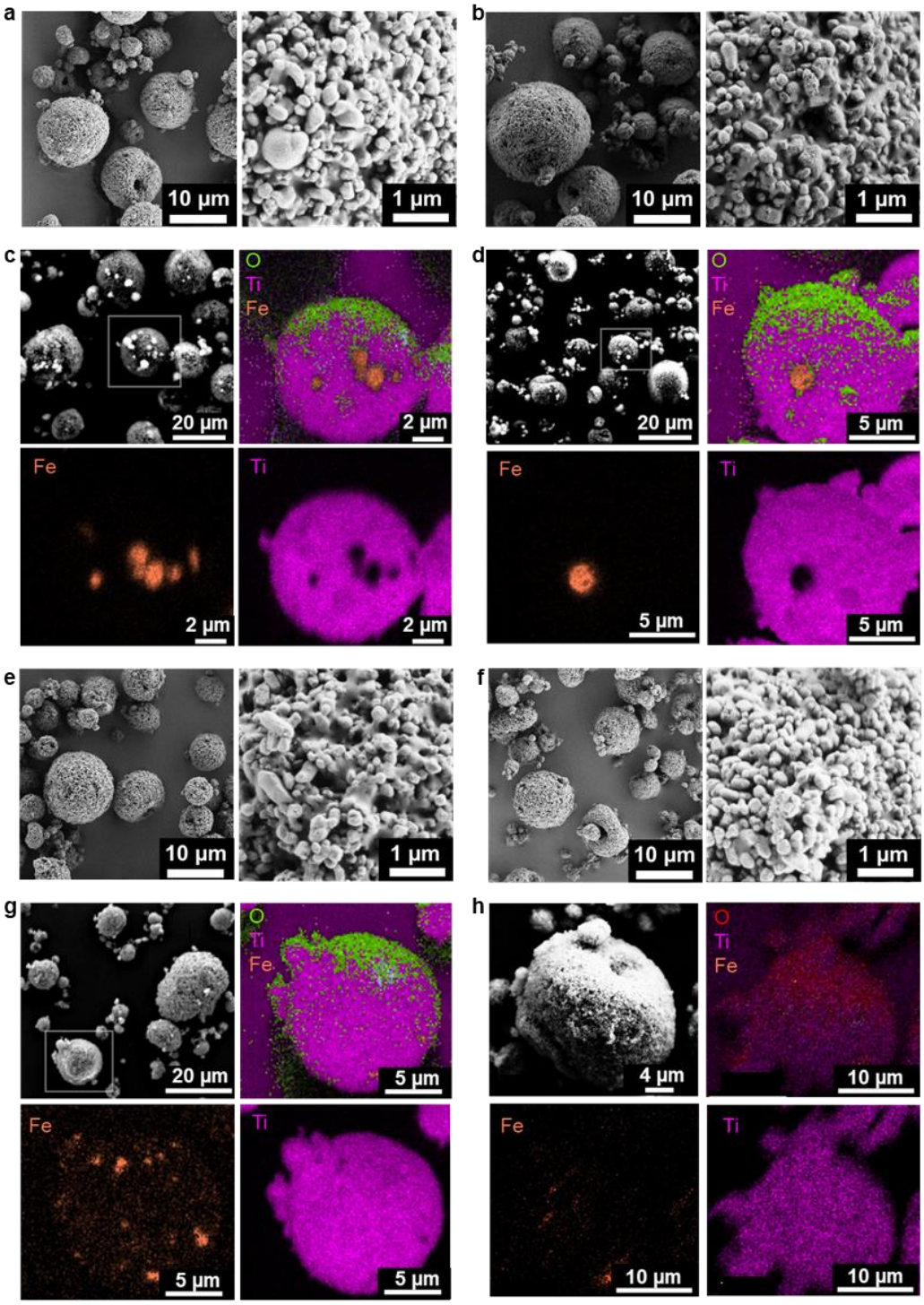

Figure S4. Scanning electron microscopy of white micro magnets. Scanning electron micrographs (a, b, e, f) and scanning electron micrographs in combination with energy dispersive X-ray spectroscopy (EDX, b, c, g, h) of α-iron containing (a-d) and iron oxide (e-h) containing white micro magnet after the 1st (a, c, e, g) and 2nd spray-drying cycle (b, d, f, h) with TiO_2.

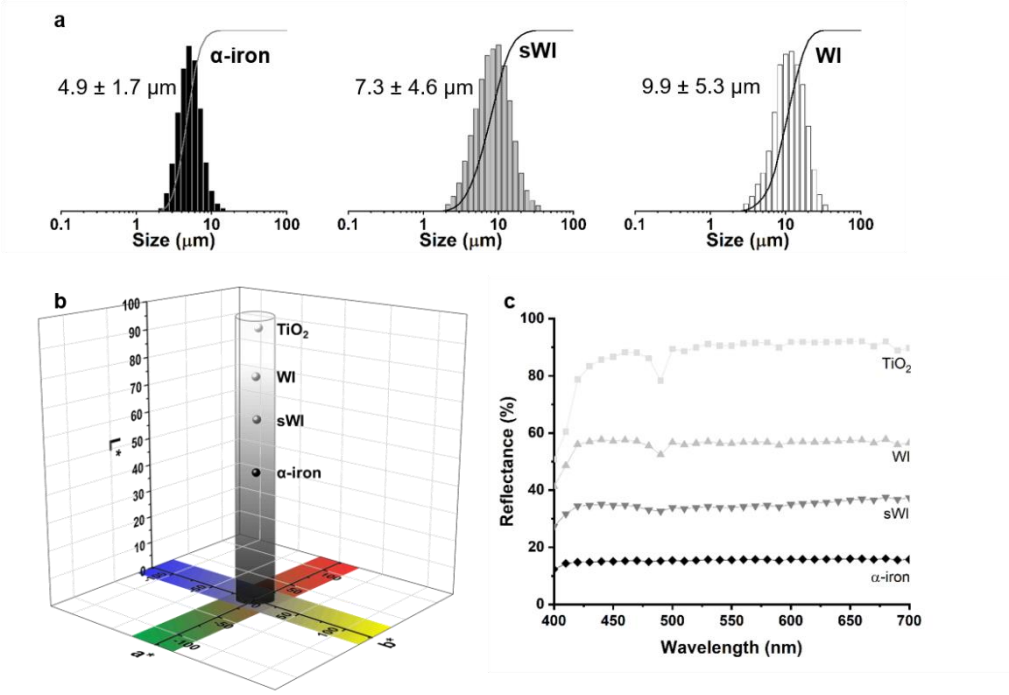

Figure S5. Particle size and color appearance of α-iron containing white micro magnet. (a) The mean particle size and standard deviation obtained from laser diffraction measurements of pure α-iron core material, α-iron containing white micro magnet after first (sWI) and second (WI) spray-drying cycle with TiO_2. (b) CIE L*a*b* values and (c) reflectivity of α-iron containing white micro magnet after first (sWI) and second (WI) spray-drying cycle compared to pure α-iron core material and titania pigment (TiO_2).

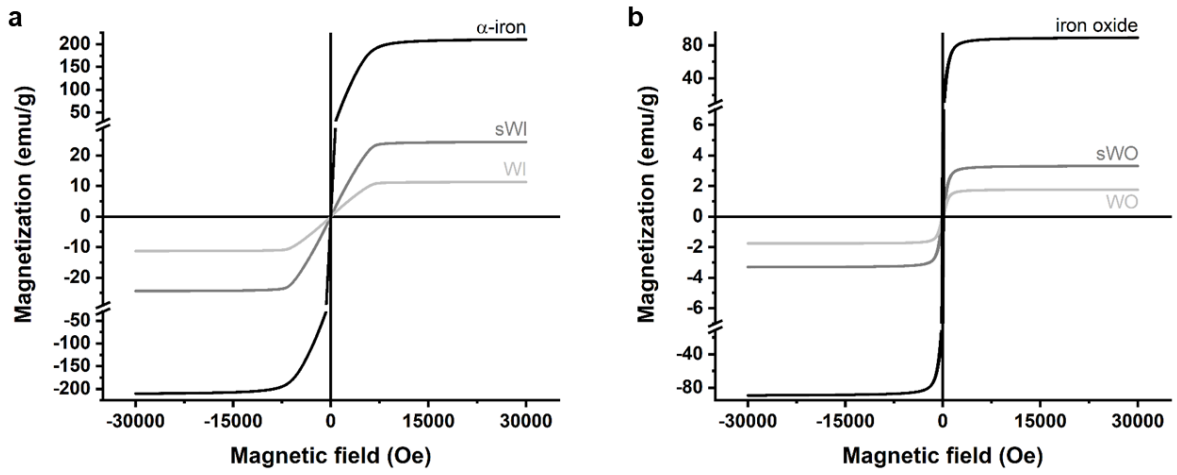

Figure S6. Magnetic properties of white micro magnets. Magnetization measurements of (a) α-iron containing and (b) iron oxide containing white micro magnet after the 1st (sWI and sWO) and 2nd spray-drying cycle with TiO_2 (WI and WO) compared to pure core materials.

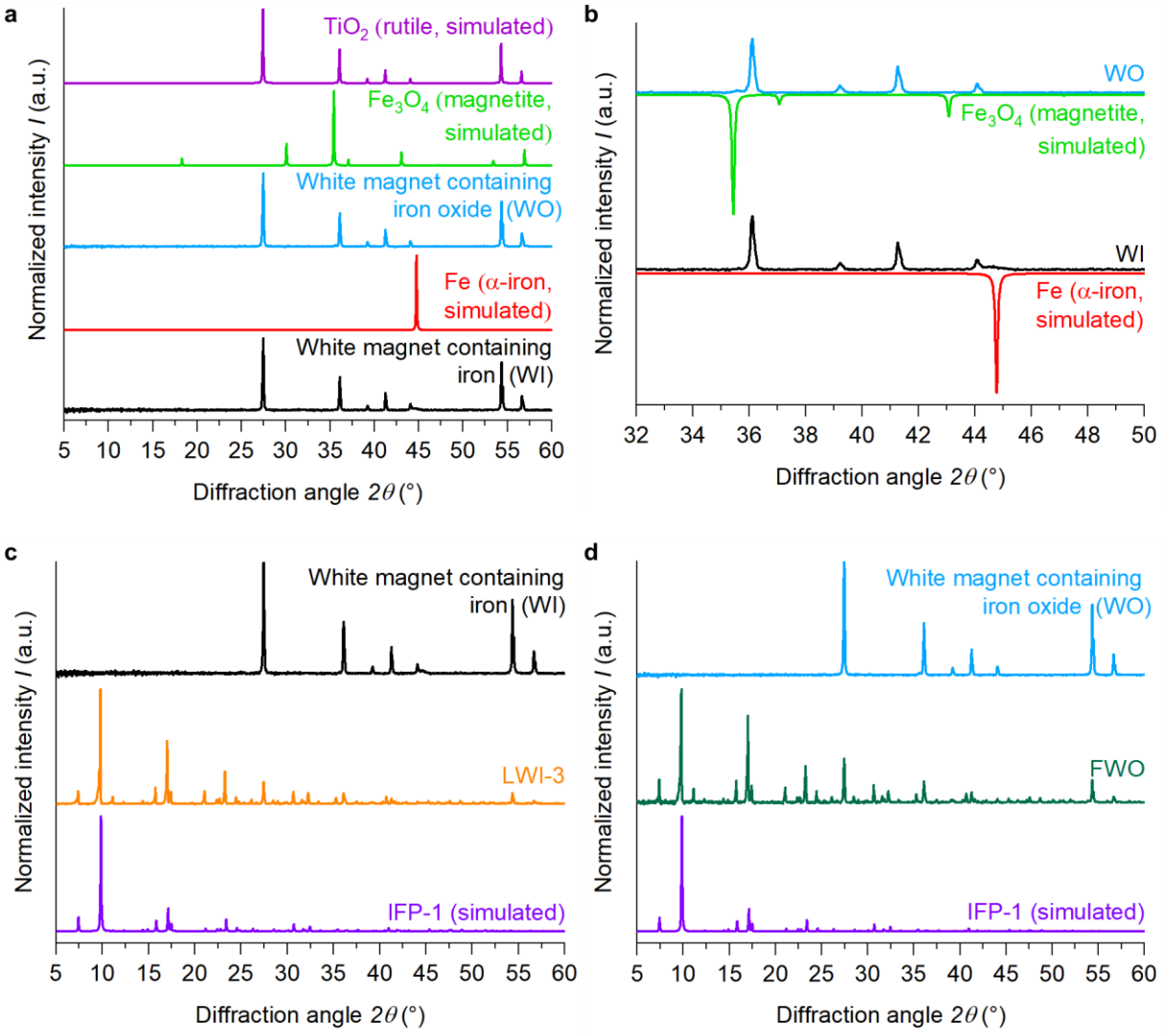

Figure S7. Powder X-ray diffraction patterns (a) and a detailed comparison (b) of α-iron containing white micro magnet (WI) and iron oxide containing white micro magnet (WO) in comparison to simulated powder X-ray diffraction patterns of rutile[1], α-iron[2] and magnetite[3], as well as powder X-ray diffraction patterns of LWI-3 (c) and LWO (d) in comparison to the pattern of WI and WO, respectively, and the simulated diffraction pattern of IFP-1.[4]

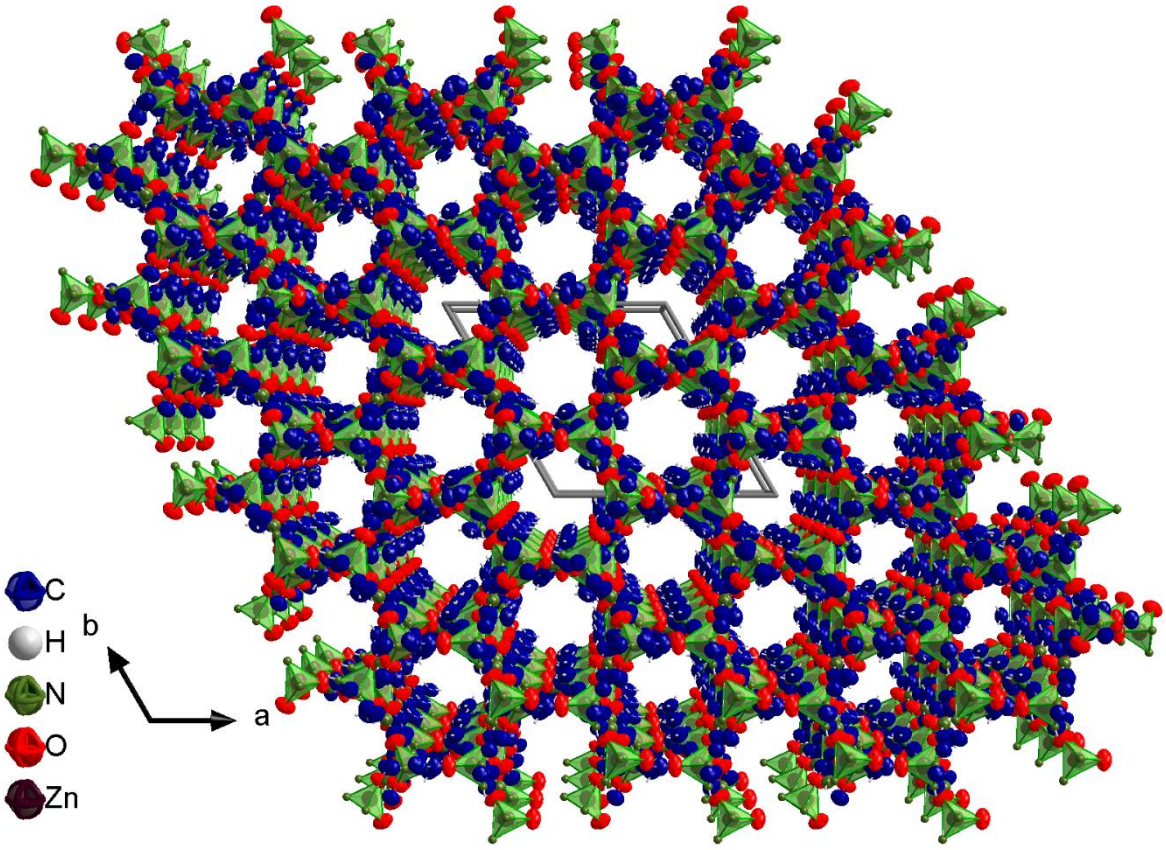

Figure S8. Perspective excerpt of the crystal structure of IFP-1[4] along the crystallographic c-axis.

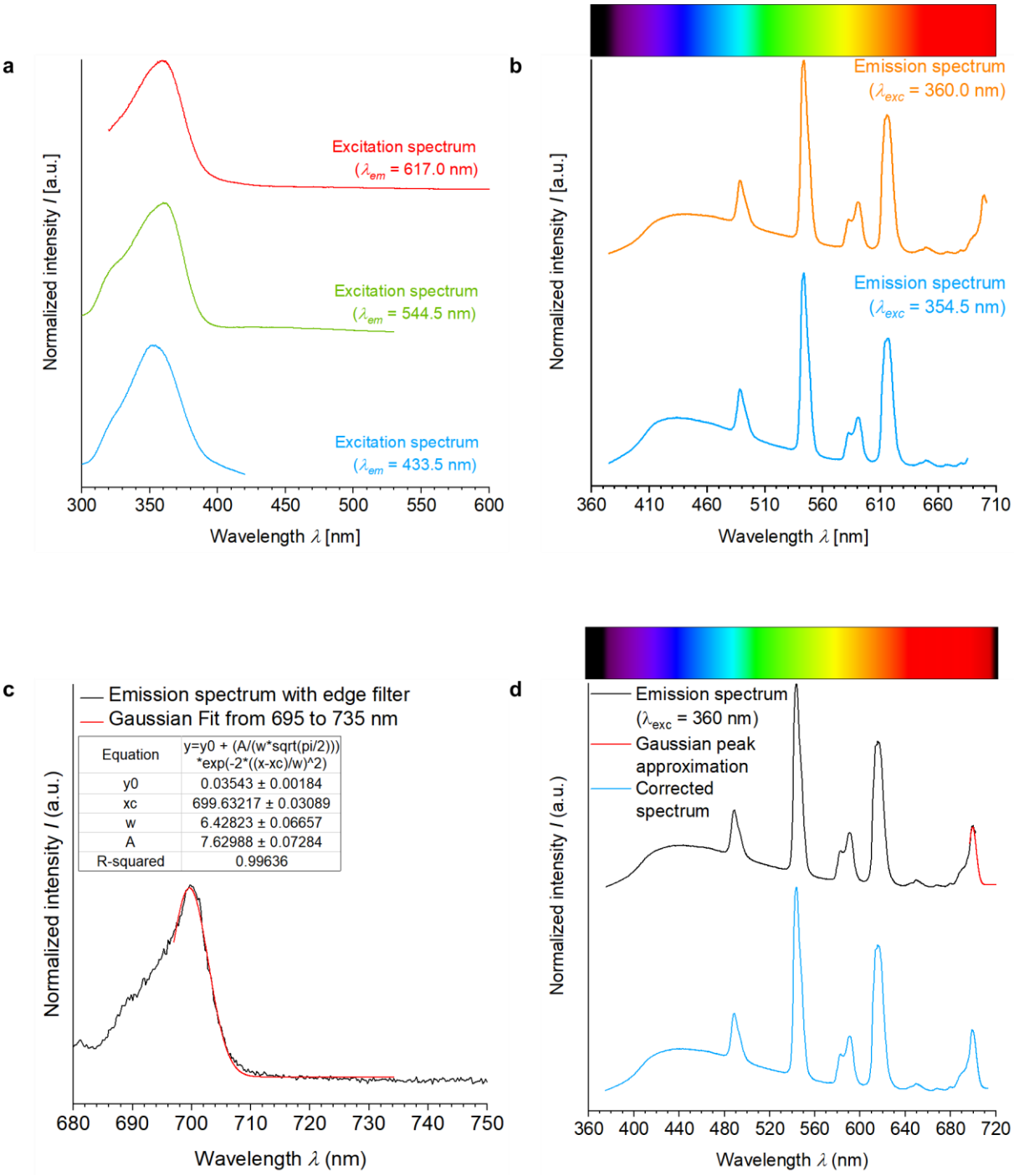

Figure S9. Excitation spectra (a) and emission spectra (b) of LWI-3. λ_{em}: emission wavelength, λ_{exc}: excitation wavelength. (c) Fitted emission spectra (λ_{exc} = 360 nm) of LWI-3. Black: spectrum as measured; red: Gaussian approximation for the rearmost europium emission band based on the Gaussian fit (d) of an emission spectrum (λ_{exc} = 363 nm) measured with an edgefilter (Newport).

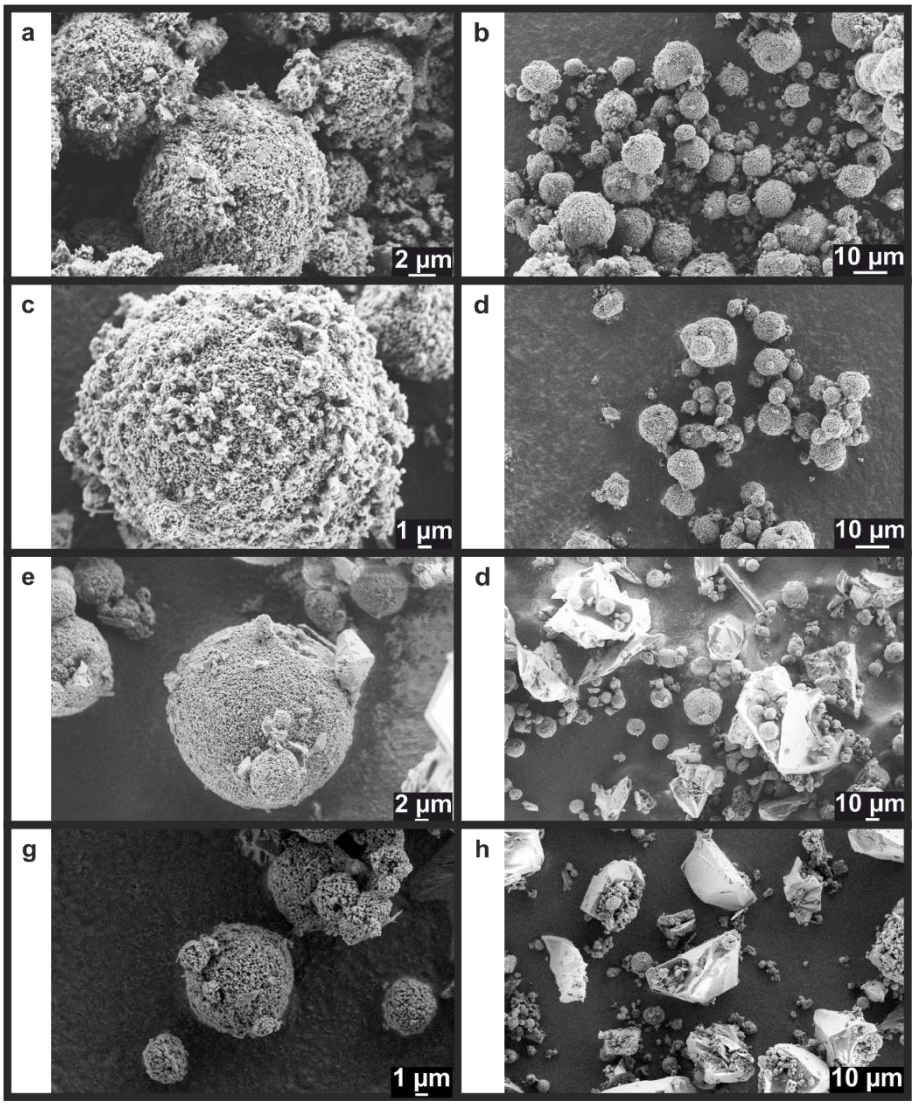

Figure S10. Electron micrographs of functionalized WI after (a, b) 1 h (LWI-1), (c, d) 3 h (LWI-2), and (e, f) 72 h (LWI-3) reaction time at 90 °C as well as electron micrographs of functionalized WO after (g, h) 72 h reaction time at 90 °C (LWO). The set-up of the composite goes from MOF crystallites of an approximate size of 1 – 3 µm in diameter as coating on magnetic particles (a – d) to magnetic particles on top of MOF crystallites of an approximate size of 50 – 70 µm in diameter (e – h) depending on the reaction time.

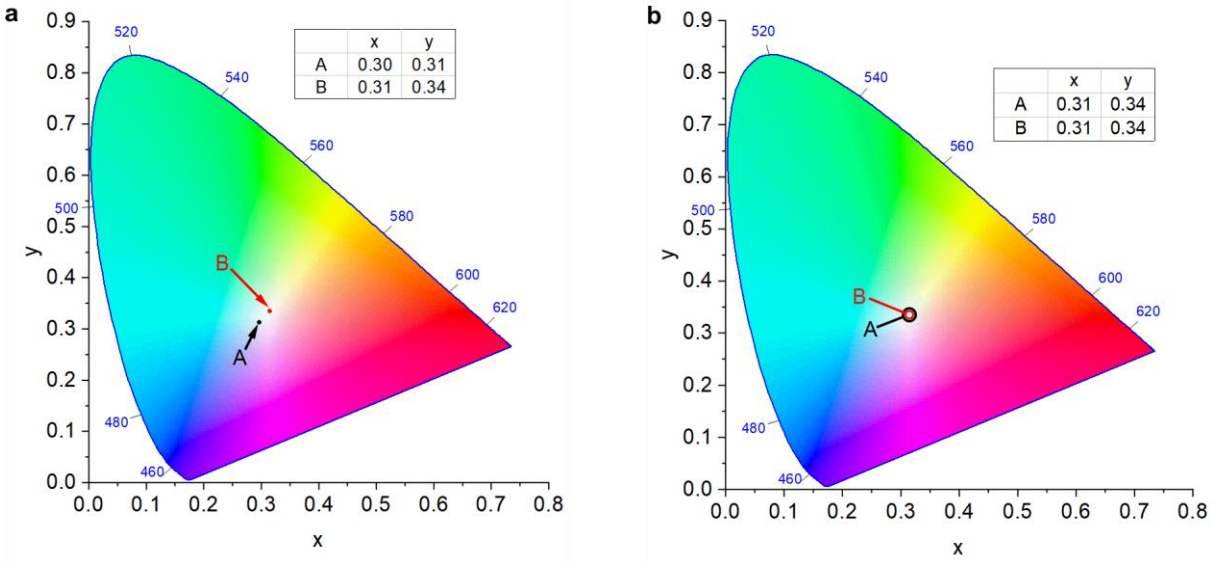

Figure S11. (a) Comparison of the chromaticity coordinates of LWI-3 in dependence of the excitation wavelength for λ_{exc} = 354 nm (A, black) and λ_{exc} = 360 nm (B, red) giving cold (A, black) as well as warm white light (B, red). (b) Comparison of the chromaticity coordinates of LWI-3 for the emission spectrum (λ_{exc} = 360 nm) as measured (A, black) as well as the emission spectrum with approximated rearmost europium emission band using a Gaussian fit (B, red) (for corresponding spectra, see Figure S9 a, b).

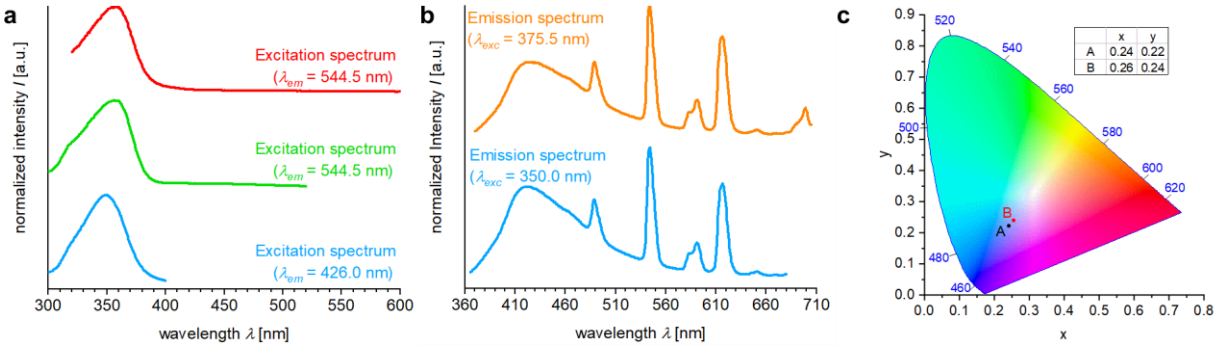

Figure S12. Excitation (a) and emission spectra (b) of LWO. λ_{em}: emission wavelength, λ_{exc}: excitation wavelength, as well as the comparison of the chromaticity coordinates of LWO (c) in dependence of the excitation wavelength for (A, black) λ_{exc} = 350 nm and (B, red) λ_{exc} = 375 nm.

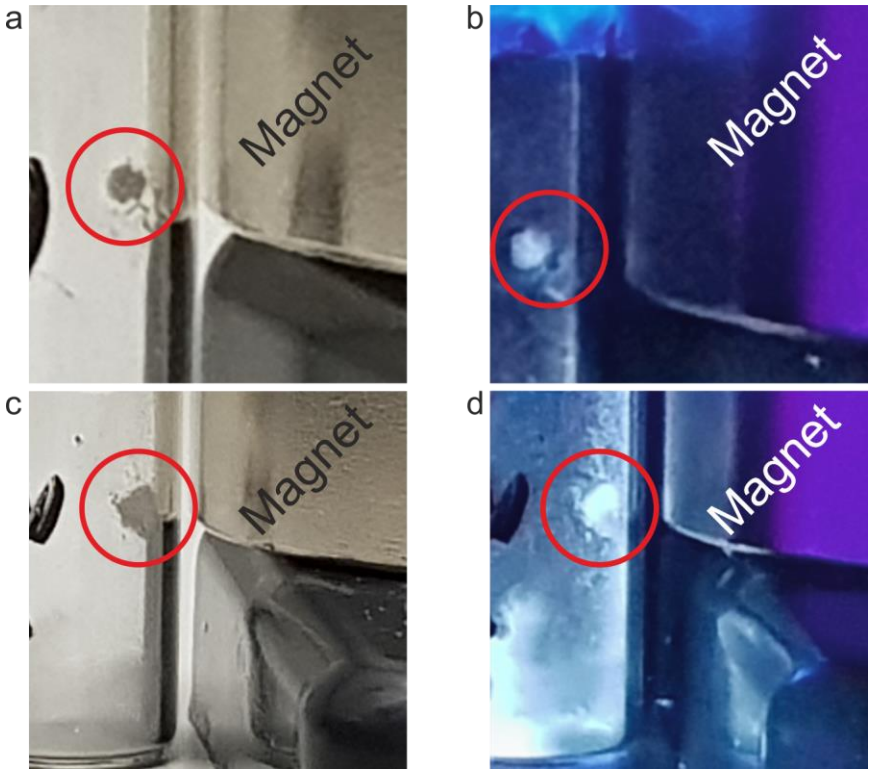

Figure S13. Visualization of white magnet particles containing α-iron (WI), functionalized with white luminescent EuTb@IFP-1 (LWI) after a reaction time of (a, b) 1 h (LWI-1) and (c, d) 3 h (LWI-2), attracted by a magnet under visible light (a, c) and under UV light excitation (λ = 365 nm; c, d).

Additional Experimental Section

Functionalization of white micro magnets with metal-organic frameworks.

For the preparation of luminescent white magnetic composite materials containing iron as magnetic component (LWI) the influence of various solvothermal reaction times was investigated. The resulting products are assigned with numbers depending on the solvothermal reaction time to illustrate these differences in reaction times and other parameters according to the designations listed in Table 1.

Table S1. Product designations of luminescent white magnets.

white magnet particle	EuTb @IFP-1	mass ratio (emitter:particle)	solvent volume	reaction time at 90 °C [h]	product designation
10.0 mg WI	5.0 mg	1:2	0.1 mL	1	LWI-1
10.0 mg WI	5.0 mg	1:2	0.1 mL	3	LWI-2
11.6 mg WI	25.1 mg	2.16:1	0.7 mL	72	LWI-3
14.3 mg WO	25.5 mg	1.79:1	0.7 mL	72	LWO

The following synthesis was performed for the product designated as LWI-3. The preparation of all other products (LWI-1, -2, and LWO) were performed analogous to this procedure with the reagent mass ratios and reaction times stated in Tab. S1. 0.5 eq. of terbium and europium ions were intercalated in-situ into the pores of IFP-1 from DMF solution. The components (WI and EuTb@IFP-1) were mixed in an agate mortar under inert atmosphere in a mass ratio of 2.16:1 (25.1 mg EuTb@IFP-1, 11.6 mg WI). After transferring the mixture into a Duran® glass ampoule and adding dry hexane (0.7 mL), the solvent was degassed by freezing the mixture, evacuating the ampoule and allowing the mixture to thaw again. This procedure was repeated one more time followed by freezing the reaction mixture, evacuating the ampoule and closing it by melting. The reaction mixture was allowed to warm up to room temperature and was homogenized in an ultrasonic bath for three minutes. Subsequently, the ampoule was placed in a corundum oven, which was heated up to 90 °C in four hours. This temperature was held constant for 72 hours before cooling to room temperature in four hours again. The solvent was removed manually under inert atmosphere and the product was dried in vacuo. After the synthesis the white luminescent, magnetic composites were magnetically separated from excess non-magnetic reactants.

For the synthesis of LWI-1 and LWI-2 the ampoules were placed in a preheated Büchi glass oven (Type GKR 50) for 1 h (LWI-1) or, respectively, 3 h (LWI-2). The synthesis of LWO was performed analogous to the synthesis of LWI. The resulting products are, depending on the reaction time, referred to the designations as listed in Tab. S1. MOF contact of WI and EuTb@IFP-1 at 90 °C for one hour (LWI-1) leads to a functionalization of the magnetic particles with MOF crystallites of an approximate size of 1 – 2 µm (Figure S10 a, b). A reaction time of three hours (LWI-2) increases the amount of MOF crystallites on top of the magnetic particles Figure S10 c, d). Keeping the temperature at 90 °C for three days (LWI-3) results in MOF crystallites of an approximate size of 2 – 3 µm on top of the magnetic particles. In addition, larger MOF crystallites (50 – 70 µm) are functionalized by the particles, too (Figure S10 e, f). This functionalization mode is also observable for LWO (Figure S10 g, h).

References

1 W. H. Baur and A. A. Khan, *Acta Crystallogr., Sect. B: Struct. Crystallogr. Cryst. Chem.*, 1971, **27**, 2133–2139.

2 E. A. Owen and G. I. Williams, *J. Sci. Instrum.*, 1954, **31**, 49–54.

3 M. E. Fleet, *Acta Crystallogr., Sect. B: Struct. Crystallogr. Cryst.*, 1981, **37**, 917–920.

4 F. Debatin, A. Thomas, A. Kelling, N. Hedin, Z. Bacsik, I. Senkovska, S. Kaskel, M. Junginger, H. Müller, U. Schilde, C. Jäger, A. Friedrich and H.-J. Holdt, *Angew. Chem., Int. Ed.*, 2010, **49**, 1258–1262.